

# Note on the thermodynamic Bethe Ansatz approach to the quantum phase diagram of the strong coupling ladder compounds

M.T. Batchelor<sup>†</sup>, X.-W. Guan<sup>†</sup>, A. Foerster<sup>‡</sup> and H.-Q. Zhou<sup>‡‡</sup>

<sup>†</sup> Department of Theoretical Physics, Research School of Physical Sciences and Engineering & Centre for Mathematics and its Applications, Mathematical Sciences Institute, Australian National University, Canberra ACT 0200, Australia

<sup>‡</sup> Instituto de Física da UFRGS, Av. Bento Gonçalves 9500, Porto Alegre, RS - Brazil

<sup>‡‡</sup> Centre for Mathematical Physics, University of Queensland, Queensland 4072, Australia

**Abstract.** We investigate the low-temperature phase diagram of the exactly solved  $su(4)$  two-leg spin ladder as a function of the rung coupling  $J_{\perp}$  and magnetic field  $H$  by means of the thermodynamic Bethe Ansatz (TBA). In the absence of a magnetic field the model exhibits three quantum phases, while in the presence of a strong magnetic field there is no singlet ground state for ferromagnetic rung coupling. For antiferromagnetic rung coupling, there is a gapped phase in the regime  $H < H_{c1}$ , a fully polarized gapped phase for  $H > H_{c2}$  and a Luttinger liquid magnetic phase in the regime  $H_{c1} < H < H_{c2}$ . The critical behaviour derived using the TBA is consistent with the existing experimental, numerical and perturbative results for the strong coupling ladder compounds. This includes the spin excitation gap and the critical fields  $H_{c1}$  and  $H_{c2}$ , which are in excellent agreement with the experimental values for the known strong coupling ladder compounds  $(5\text{IAP})_2\text{CuBr}_4 \cdot 2\text{H}_2\text{O}$ ,  $\text{Cu}_2(\text{C}_5\text{H}_{12}\text{N}_2)_2\text{Cl}_4$  and  $(\text{C}_5\text{H}_{12}\text{N})_2\text{CuBr}_4$ . In addition we predict the spin gap  $\Delta \approx J_{\perp} - \frac{1}{2}J_{\parallel}$  for the weak coupling compounds with  $J_{\perp} \sim J_{\parallel}$ , such as  $(\text{VO})_2\text{P}_2\text{O}_7$ , and also show that the gap opens for arbitrary  $J_{\perp}/J_{\parallel}$ .

PACS numbers: 75.10.Jm, 64.40.Cn

Recently there has been considerable theoretical and experimental interest in spin ladder systems. With the rapid progress presently being made in nano-engineering, many compounds with a ladder structure have been experimentally realized, such as  $\text{SrCu}_2(\text{BO}_3)_2$ ,  $\text{Cu}_2(\text{C}_5\text{H}_{12}\text{N}_2)_2\text{Cl}_4$ ,  $(\text{C}_5\text{H}_{12}\text{N})_2\text{CuBr}_4$  and  $\text{KCuCl}_3$  [1]. The existence of a spin gap, magnetization plateaus, superconductivity under hole doping, etc, are examples of some interesting physical properties that may be observed in experiments involving ladder compounds (see, e.g., Refs [1]-[7] and references therein). From the theoretical point of view, most of the results for ladder systems were initially obtained from studies of the standard Heisenberg ladder, which in contrast to its one-dimensional counterpart, cannot be solved exactly. Subsequently, other generalised ladder models have been proposed [8] and analysed through various numerical, approximate and exact approaches [9, 10, 11, 12].

On the other hand, although some exactly solved or integrable ladder models have been introduced [13, 14, 15], none have been used to predict physical properties which could be compared directly with experimental data, such as the critical magnetic fields. In this context, the integrable spin ladder model based on the  $su(4)$  algebra [13] appears to be a good candidate for this purpose, since its Hamiltonian consists of the standard Heisenberg ladder model with an extra biquadratic spin interaction term along the legs, the physical importance of which has been noted [8]. In the strong coupling limit, the contribution to the low-temperature physics from the biquadratic term is minimal, and as a consequence, the model exhibits similar critical behavior to the standard Heisenberg ladder. Therefore it is reasonable to expect that the integrable  $su(4)$  ladder model can well describe the low-temperature critical behavior of the strong coupling ladder materials. In addition, by properly minimizing the intrachain coupling in the integrable ladder Hamiltonian, the model may also be used to describe the weak coupling compounds.

Here we show that this is in fact true in the strong coupling regime by investigating the quantum phase diagram of the integrable  $su(4)$  ladder, which can be tested by experiments. Our analytic expression for the gap,  $\Delta = J_\perp - 4J_\parallel/\gamma$ , and the critical fields,  $\mu_B g H_{c1} = \Delta$  and  $\mu_B g H_{c2} = J_\perp + 4J_\parallel/\gamma$ , where  $\gamma$  is a rescaling constant, can be applied in general to strong coupling ladder compounds with Heisenberg interactions, such as  $(5\text{IAP})_2\text{CuBr}_4 \cdot 2\text{H}_2\text{O}$ ,  $\text{Cu}_2(\text{C}_5\text{H}_{12}\text{N}_2)_2\text{Cl}_4$ ,  $(\text{C}_5\text{H}_{12}\text{N})_2\text{CuBr}_4$  and  $\text{KCuCl}_3$ , by choosing  $\gamma \approx 4$ . For weak ( $J_\perp \sim J_\parallel$ ) coupling compounds, such as  $(\text{VO})_2\text{P}_2\text{O}_7$ , the choice  $\gamma \approx 8$  determines a good fit for the gap [1, 16]. In addition, in the presence of a strong magnetic field, we shown that the quantum phase diagram and the critical behavior predicted from the thermodynamic Bethe Ansatz (TBA) are in a good agreement with the experimental results for the above-mentioned compounds. We also show that the gap opens for an arbitrary value of  $J_\perp/J_\parallel$ , in accordance with the experimental results.

**I. The Model.** We consider the phase diagram of the simplest integrable spin ladder

[13]

$$H = \frac{J_{\parallel}}{\gamma} H_{\text{leg}} + J_{\perp} \sum_{j=1}^L \vec{S}_j \vec{T}_j + h \sum_{j=1}^L (S_j^z + T_j^z), \quad (1)$$

where

$$H_{\text{leg}} = \sum_{j=1}^L \left( \vec{S}_j \vec{S}_{j+1} + \vec{T}_j \vec{T}_{j+1} + 4 \vec{S}_j \vec{S}_{j+1} \vec{T}_j \vec{T}_{j+1} \right). \quad (2)$$

Here  $\vec{S}_j$  and  $\vec{T}_j$  are the standard spin- $\frac{1}{2}$  operators acting on site  $j$  of the upper and lower legs, respectively,  $J_{\parallel}$  and  $J_{\perp}$  are the intra (leg) and interchain (rung) couplings and  $h$  is the magnetic field. Throughout,  $L$  is the number of rungs and periodic boundary conditions are imposed. Essentially, the competition between the rung and leg couplings and the magnetic field  $h$  determines the physical properties and the critical behavior of the system. In order to facilitate the comparison with real compounds, the intrachain part of this model (2) can be minimized through a rescaling constant  $\gamma$ . In comparison with the standard spin- $\frac{1}{2}$  Heisenberg ladder [1, 2, 3, 17], the above Hamiltonian contains a four-spin interaction term, which minimizes the Haldane phase [8] and causes a shift of the critical value of the rung coupling  $J_{\perp}$  at which the model becomes massive. It is well established that this Hamiltonian is integrable and its leg part  $H_{\text{leg}}$  is (up to a constant) simply the permutation operator corresponding to the  $su(4)$  algebra [13]. In addition, after the convenient change of basis,  $|1\rangle = \frac{1}{\sqrt{2}} (|\uparrow\downarrow\rangle - |\downarrow\uparrow\rangle)$ ,  $|2\rangle = |\uparrow\uparrow\rangle$ ,  $|3\rangle = \frac{1}{\sqrt{2}} (|\uparrow\downarrow\rangle + |\downarrow\uparrow\rangle)$ ,  $|4\rangle = |\downarrow\downarrow\rangle$ , where the first state denotes the rung singlet and the three others the components of the triplet, the leg part remains of the same form while the rung term becomes diagonal. This rung term reduces the  $su(4)$  symmetry of  $H_{\text{leg}}$  to  $su(3) \oplus u(1)$  symmetry. Switching on the magnetic field breaks this symmetry further due to Zeeman splitting. This Hamiltonian can be diagonalized using the nested algebraic Bethe Ansatz (BA) with three levels. It is worth noting that for the ladder Hamiltonian (1), the singlet rung state is energetically favoured for  $J_{\perp} > 0$ , whereas the triplet rung state is favoured for  $J_{\perp} < 0$ . On applying the magnetic field, component  $|2\rangle$  of the triplet is energetically favoured. We will use these properties to our advantage by doing calculations with the choice of ordering for which the BA reference state is the closest to the true groundstate of the system.

The underlying BA equations for Hamiltonian (1) are well known [18] and consist of a set of three coupled equations depending on the flavors,  $v$ ,  $u$  and  $w$ . Adopting the string conjecture [19, 20] and taking the thermodynamic limit, the densities of the three flavors,  $\rho_n^{(1)}(v)$ ,  $\rho_n^{(2)}(u)$  and  $\rho_n^{(3)}(w)$ , can be defined as usual. After some manipulations, the BA equations reduce to

$$\begin{pmatrix} \ln(1 + \eta_n^{(1)}) \\ \ln(1 + \eta_n^{(2)}) \\ \ln(1 + \eta_n^{(3)}) \end{pmatrix} = \frac{G}{T} + K * \begin{pmatrix} \ln(1 + \eta_m^{(1)-1}) \\ \ln(1 + \eta_m^{(2)-1}) \\ \ln(1 + \eta_m^{(3)-1}) \end{pmatrix}, \quad (3)$$

where  $\rho_n^{(1)h}(v)$ ,  $\rho_n^{(2)h}(u)$  and  $\rho_n^{(3)h}(w)$  denote the hole densities and

$$K = \begin{pmatrix} \sum_m A_{nm} & -\sum_m a_{nm} & 0 \\ -\sum_m a_{nm} & \sum_m A_{nm} & -\sum_m a_{nm} \\ 0 & -\sum_m a_{nm} & \sum_m A_{nm} \end{pmatrix}, \quad (4)$$

where

$$A_{nm}(\lambda) = \delta(\lambda)\delta_{nm} + (1 - \delta_{nm})a_{|n-m|}(\lambda) + a_{n+m}(\lambda) + 2 \sum_{l=1}^{\text{Min}(n,m)-1} a_{|n-m|+2l}(\lambda), \quad (5)$$

$$a_{nm}(\lambda) = \sum_{l=1}^{\text{Min}(n,m)} a_{n+m+1-2l}(\lambda), \quad (6)$$

with  $a_n(\lambda) = \frac{1}{2\pi} \frac{n}{n^2/4 + \lambda^2}$ . The symbol  $*$  denotes convolution and  $\eta_n^{(l)}(\lambda) = \rho_n^{(l)h}(\lambda)/\rho_n^{(l)}(\lambda) := \exp(\epsilon_n^{(l)}(\lambda)/T)$ ,  $l = 1, 2, 3$ . The dressed energy  $\epsilon_n^{(l)}$  plays the role of an excitation energy measured from the Fermi level. The driving matrix  $G$  depends on the choice of the reference state. Explicitly, for  $J_\perp < 0$ ,  $G = \text{column}(-\frac{J_\parallel}{\gamma}2\pi a_n + nh, nh, -n(J_\perp + h))$  giving the free energy

$$\frac{F(T, h)}{L} = -h - T \int_{-\infty}^{\infty} \sum_{n=1}^{\infty} a_n(\lambda) \ln(1 + e^{-\frac{\epsilon_n^{(1)}(\lambda)}{T}}) d\lambda. \quad (7)$$

On the other hand, for  $J_\perp > 0$ ,  $G = \text{column}(-\frac{J_\parallel}{\gamma}2\pi a_n + n(J_\perp - h), nh, nh)$ , which leads to the form of the free energy (7) without the field term  $h$ . The TBA equations (3) provide a clear physical picture of the groundstate, the elementary excitations, as well as the thermodynamic quantities, such as the free energy, magnetization, susceptibility, etc. Our results extend the earlier calculations on this model [13, 21].

**II. Ferromagnetic rung coupling.** In the low-temperature regime  $T \rightarrow 0$ , only the negative part of the dressed energies  $\epsilon^{(l)}$ , denoted by  $\epsilon^{(l)-}$ , contribute to the ground-state energy. The TBA equations (3) then become

$$\begin{aligned} \epsilon^{(1)} &= g_1 - a_2 * \epsilon^{(1)-} + a_1 * \epsilon^{(2)-}, \\ \epsilon^{(2)} &= g_2 - a_2 * \epsilon^{(2)-} + a_1 * [\epsilon^{(1)-} + \epsilon^{(3)-}], \\ \epsilon^{(3)} &= g_3 - a_2 * \epsilon^{(3)-} + a_1 * \epsilon^{(2)-}, \end{aligned} \quad (8)$$

where  $g_a$ ,  $a = 1, 2, 3$ , are the driving terms with respect to the basis order. In the regime  $J_\perp < 0$ , the component  $|\uparrow\uparrow\rangle$  of the triplet state is chosen as the reference state. The driving terms are given by  $g_1 = -\frac{J_\parallel}{\gamma}2\pi a_1 + h$ ,  $g_2 = h$  and  $g_3 = -h - J_\perp$ , respectively. Thus, in the absence of a magnetic field, the triplet is completely degenerate. The Fermi surface of the singlet is lifted as  $J_\perp$  becomes more negative. If  $J_\perp$  is negative enough, the singlet rung state is not involved in the groundstate, namely  $\epsilon^{(3)}(0) \geq 0$ , whereas the two other triplet Fermi seas still have their Fermi boundaries at infinity. In such a configuration, we may determine the critical point defining the transition from the  $su(4)$  phase into the  $su(3)$  phase by solving the TBA equations

(8), with result  $J_c^- = -\frac{J_{\parallel}}{\gamma}(\frac{\pi}{\sqrt{3}} - \ln 3)$ . At this critical point the free energy is given by  $\frac{F(0,0)}{L} \approx -\frac{2J_{\parallel}}{3\gamma}(\psi(1) - \psi(\frac{1}{3}))$ , indicating a standard  $su(3)$  phase. Here  $\psi(n)$  is the digamma function. It is worth noting that the critical point  $J_c^-$  does not stabilize if an external magnetic field is applied. If the magnetic field is large enough, the ferromagnetic state  $|\uparrow\uparrow\rangle$  becomes the true physical groundstate, i.e., there is a fully polarized gapped phase. It is found that for  $h \geq H_c^F = \frac{4J_{\parallel}}{\gamma}$ , the state is fully-polarized provided that  $J_{\perp} \leq -\frac{4J_{\parallel}}{\gamma}$ . Therefore, in the ferromagnetic regime, the groundstate is in the critical  $su(3)$  phase. If the magnetic field is greater than  $H_c^F$ , the groundstate is ferromagnetic with a magnetization plateau  $S^z = 1$ .

**III. Strong antiferromagnetic regime.** In the antiferromagnetic regime,  $J_{\perp} > 0$ , the rung singlet state is the reference state. Thus the driving terms are given by  $g_1 = -\frac{J_{\parallel}}{\gamma}2\pi a_1 + J_{\perp} - h$  and  $g_2 = g_3 = h$ , respectively. From the TBA equations (8), if  $h = 0$  we immediately conclude that the triplet excitation is massive with the gap given by  $\Delta = J_{\perp} - 4J_{\parallel}/\gamma$  for the regime  $J_{\perp} \geq J_c^+ = \frac{4J_{\parallel}}{\gamma}$ . Here  $J_c^+$  is the critical point at which the quantum phase transition from the three branches of the Luttinger liquid phase to the dimerized  $u(1)$  phase occurs. To obtain good agreement with the experimental gap, we fix the rescaling constant  $\gamma$  with the coupling constants remaining arbitrary. For the strong coupling compounds, e.g.,  $(5\text{IAP})_2\text{CuBr}_4 \cdot 2\text{H}_2\text{O}$  [5],  $\text{Cu}_2(\text{C}_5\text{H}_{12}\text{N}_2)_2\text{Cl}_4$  [3],  $(\text{C}_5\text{H}_{12}\text{N})_2\text{CuBr}_4$  [4], the experimental gap is well established as  $\Delta \approx J_{\perp} - J_{\parallel}$ , and as a consequence, we fix  $\gamma \approx 4$ . On the other hand, for weak coupling compounds, e.g.,  $(\text{VO})_2\text{P}_2\text{O}_7$  [1, 16], the choice  $\gamma \approx 8$  determines a good fit with the gap  $\Delta \approx \frac{1}{2}J_{\perp}$ . We stress that the purpose of introducing the rescaling constant is to minimize the effects of the biquadratic term, so that the model lies in the same Haldane phase as the pure Heisenberg ladder.

**IV. Magnetization plateau.** The phase diagram of the antiferromagnetic spin ladders in the presence of a magnetic field is particularly interesting, because the critical points can be measured through critical magnetic fields. The appearance of quantized magnetization plateaus in the presence of a strong magnetic field is expected on general grounds [1]. From the TBA equations (8) for antiferromagnetic rung coupling we observe that the magnetic field lifts the Fermi seas of  $\epsilon^{(2)}$  and  $\epsilon^{(3)}$ . If  $J_{\perp} > J_c^+$ , we can show that the two components of the triplet states,  $|3\rangle$  and  $|4\rangle$ , do not become involved in the groundstate for a strong magnetic field. Basically, the magnetic field lifts the component  $|2\rangle$  of the triplet closer to the singlet groundstate such that they form a new effective spin- $\frac{1}{2}$  state. Therefore, in a strong magnetic field the groundstate may be considered as a condensate of  $su(2)$  hard-core bosons. The gap can be deduced via the magnetic field  $h$ : the first critical field occurs at  $H_{c1}$  where  $g\mu_B H_{c1} = \Delta$ , i.e. the magnetic field closes the gap. The quantum phase transition from a gapped to a gapless Luttinger phase occurs. However, by continuing to increase the magnetic field  $h$  above the first critical field  $H_{c1}$ , the component  $|2\rangle$  of the triplet becomes involved in the groundstate with a finite susceptibility. If the magnetic field is greater than the rung coupling, i.e.  $h > J_{\perp}$ , the

state  $|2\rangle$  becomes the lowest level. Therefore, it is reasonable to choose the basis order as  $(|2\rangle, |1\rangle, |3\rangle, |4\rangle)^T$ . Subsequently the driving terms are given by  $g^{(1)} = -2\pi J_{\parallel} a_1 - J_{\perp} + h$ ,  $g^{(2)} = J_{\perp}$  and  $g^{(3)} = h$ . From the TBA, we see that the groundstate is a fully-polarized ferromagnetic state when the magnetic field is greater than  $H_{c2} = J_{\perp} + \frac{4J_{\parallel}}{\gamma}$ . Indeed, the critical field  $H_{c2}$  is in excellent agreement with the experimental data for the very strong coupling compound  $(5\text{IAP})_2\text{CuBr}_4 \cdot 2\text{H}_2\text{O}$  (abbreviated as B5i2aT), [5] and in a good agreement with the strong coupling compounds  $\text{Cu}_2(\text{C}_5\text{H}_{12}\text{N}_2)_2\text{Cl}_4$  (abbreviated Cu(Hp)Cl) [3] and  $(\text{C}_5\text{H}_{12}\text{N})_2\text{CuBr}_4$  (abbreviated BPCN) [4] (see Table 1). On the other hand, the precise structure of the compound  $\text{KCuCl}_3$  is not clear [1]. It is believed to exhibit a double-chain structure [6] with a gap  $\Delta \approx 35K$  identified via the best fitting in the susceptibility curve through the Troyer formula [22]. The coupling constants are determined as  $J_{\perp} = 4J_{\parallel}$ ,  $J_{\parallel} = 12.3K$ ,  $J_{\text{diag}} = 0$  [6]. However, high-field measurements indicate the gap  $\Delta \approx 31.1K$  [7]. Our TBA result gives poor agreement with the experimental result for this type of ladder compound (see Table 1). This suggests that the compound may exhibit a double-chain structure with additional diagonal interaction. For these double-chain structure ladders, such as  $\text{KCuCl}_3$ ,  $\text{TlCuCl}_3$  etc., the leg couplings appear to be very large, resulting in discrepancy with the critical fields derived from the TBA method.

After a similar calculation, we obtain the magnetization  $S^z \approx 4Q_1(1 - 2Q_1/\pi)/\pi$  in the vicinity of the critical field  $H_{c1}$ , with the Fermi boundary  $Q_1 \approx \sqrt{(h - H_{c1})/(H_{c1} - 5h)}$ . For a very strong magnetic field such that  $H_{c2} - h \ll 1$  the free energy is

$$\frac{F(0, h)}{L} \approx -h - \frac{4(H_{c2} - h)^{\frac{3}{2}}}{\pi \sqrt{5h - H_{c2}}}, \quad (9)$$

and the susceptibility  $\kappa \approx \frac{3}{\pi\sqrt{4H_{c2}}}(H_{c2} - h)^{-\frac{1}{2}}$ , which indicates the nature of the singular behavior in a phase transition from a gapless to a ferromagnetic phase. The magnetization is given by  $S^z \approx 1 - 4Q_2(1 - 2Q_2/\pi)/\pi$ , where  $Q_2 \approx \sqrt{(H_{c2} - h)/(5h - H_{c2})}$ . The fact that the magnetization depends on the square root of the field in the vicinity of the critical fields is consistent with other theoretical [11, 12] and numerical results [9]. The magnetization increases almost linearly between the critical field  $H_{c1}$  and  $H_{c2}$ . The groundstate is ferromagnetic above  $H_{c2}$  with the gap  $\Delta = \mu g(H - H_{c2})$ .

Numerical solution of the TBA equations gives a reasonable magnetization curve (see Fig. 1) which passes through an inflection point midway between  $H_{c1}$  and  $H_{c2}$ . This inflection point is clearly visible in experimental curves, e.g. for  $(5\text{IAP})_2\text{CuBr}_4 \cdot 2\text{H}_2\text{O}$  [5],  $\text{Cu}_2(\text{C}_5\text{H}_{12}\text{N}_2)_2\text{Cl}_4$  [3] and  $(\text{C}_5\text{H}_{12}\text{N})_2\text{CuBr}_4$  [4]. The physical meaning of the inflection point is that the probabilities of the singlet and the triplet states  $|2\rangle$  in the groundstate are equal. It suggests an ordered dimer state close to half-filling [23]. Therefore, in the strong-coupling regime, the one point correlation function  $\langle S_j \cdot T_j \rangle = -\frac{3}{4}$  lies in a gapped singlet groundstate, which indicates an ordered dimer phase, while  $\langle S_j \cdot T_j \rangle = \frac{1}{4}$  is in the fully-polarized ferromagnetic phase. However, in a Luttinger liquid phase, we find

Compounds	$g$	$J_{\perp}$	$J_{\parallel}$	$\gamma$	$H_{c1}(\text{exp})$	$H_{c2}(\text{exp})$	$H_{c1}(\text{TBA})$	$H_{c2}(\text{TBA})$
B5i2aT	2.1	13K	1.15K	4	8.4T	10.4T	8.3T	10.03T
Cu(Hp)Cl	2.03	13.2K	2.5K	4	7.5T	13.2T	7.84T	11.51T
BPCB	2.13	13.3K	3.8K	4	6.6T	14.6T	6.6T	11.95T
KCuCl <sub>3</sub>	2.05	49.2K	12.3K	2.68	22.4T	$\approx 60T$	22.4T	49T

**Table 1.** Comparison between the experimental values for the critical points  $H_{c1}$  and  $H_{c2}$  for strong coupling ladder compounds and the TBA results obtained from the  $su(4)$  integrable model.

$\langle S_j \cdot T_j \rangle = -\frac{3}{4} + S^z$ . The magnetic field increases the one point correlation function.

We also notice that our results for the gap,  $\Delta = J_{\perp} - 4J_{\parallel}/\gamma$ , and the critical field,  $H_{c2} = J_{\perp} + 4J_{\parallel}/\gamma$ , coincide for  $\gamma = 4$  with the first-order perturbation theory results obtained for strong coupling [11]. However, their higher-order terms lead to poor agreement with the experimental results. It is apparent that the rescaling constant  $\gamma$  causes a shift in the critical point. This can be seen from the values of

$$H_{c2}/\Delta = 1 + 2/\left(\frac{\gamma J_{\perp}}{4J_{\parallel}} - 1\right), \quad (10)$$

which are plotted in Fig. 2. The larger the ratio of  $\frac{J_{\perp}}{J_{\parallel}}$ , the closer the two critical points are. This means that the critical points  $H_{c1}$  and  $H_{c2}$  cannot be distinguished for a very large energy gap. Once the gap is closed by an external field, the groundstate immediately becomes fully-polarized. This is evident in the strong coupling compound  $(5\text{IAP})_2\text{CuBr}_4 \cdot 2\text{H}_2\text{O}$  [5]. Here the gap opens only if  $J_{\perp}/J_{\parallel} \geq 4/\gamma$ , with  $\gamma$  arbitrary. And therefore the gap opens for arbitrary  $J_{\perp}/J_{\parallel}$ .

Finally, we show the phase diagram in the presence of a magnetic field in Fig. 3. In the ferromagnetic rung coupling regime, the fully-polarized ferromagnetic state lies in the region  $h \geq |J_{\perp}|$  and  $h \geq 4J_{\parallel}/\gamma$ , whereas the  $su(3)$  Luttinger magnetic phase is in the region  $h < |J_{\perp}|$  and left of the boundary between the  $su(3)$  and  $su(4)$  phases. The  $su(4)$  phase is in the region  $h < 4J_{\parallel}/\gamma$  and right of this boundary. In the antiferromagnetic rung coupling regime, the singlet rung state lies in  $h < J_{\perp} - 4J_{\parallel}/\gamma$  whereas the ferromagnetic fully-polarized state is in the region  $h \geq J_{\perp} + 4J_{\parallel}/\gamma$ . The  $su(2)$  magnetic phase remains in the region  $h > J_{\perp} - 4J_{\parallel}/\gamma$ ,  $h < J_{\perp} + 4J_{\parallel}/\gamma$  and  $J_{\perp} \geq 4J_{\parallel}/\gamma$ . The  $su(4)$  magnetic phase lies in the region  $h < J_{\perp} + 4J_{\parallel}/\gamma$  and  $0 < J_{\perp} < 4J_{\parallel}/\gamma$ .

To conclude, we have studied the phase diagram of the integrable  $su(4)$  spin ladder model (1) by means of the TBA. In particular, the critical behavior at the critical points  $H_{c1}$  and  $H_{c2}$  was derived. In the presence of a strong magnetic field, the phase diagram is in a good agreement with the experimental observations for the strong coupling compounds  $(5\text{IAP})_2\text{CuBr}_4 \cdot 2\text{H}_2\text{O}$  [5],  $\text{Cu}_2(\text{C}_5\text{H}_{12}\text{N}_2)_2\text{Cl}_4$  [3] and  $(\text{C}_5\text{H}_{12}\text{N})_2\text{CuBr}_4$  [4]. We have also predicted the spin gap  $\Delta \approx J_{\perp} - \frac{1}{2}J_{\parallel}$  for the weak coupling compounds with  $J_{\perp} \sim J_{\parallel}$ , such as  $(\text{VO})_2\text{P}_2\text{O}_7$  and also shown that the gap opens for arbitrary  $J_{\perp}/J_{\parallel}$ .

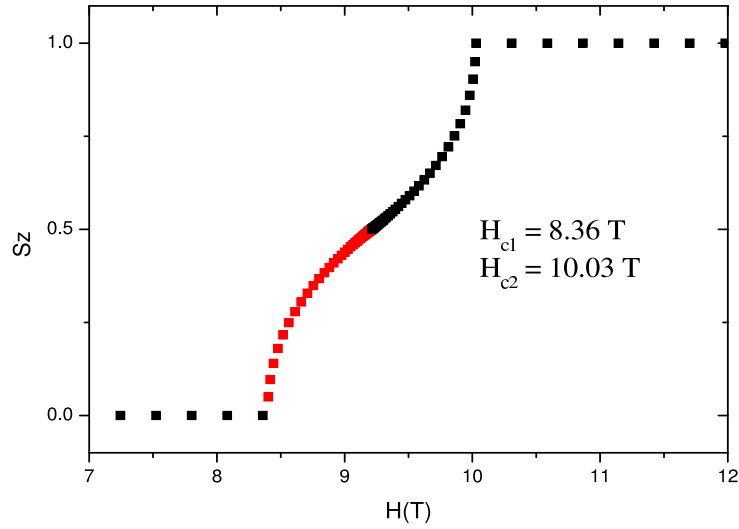


**Figure 1.** Magnetization  $S^z$  versus magnetic field  $H = \mu_B g h$  obtained from the TBA equations for the values  $J_{\perp} = 13K$ ,  $J_{\parallel} = 1.15K$  and  $\gamma = 4$  for the strong coupling compound  $(5\text{IAP})_2\text{CuBr}_4 \cdot 2\text{H}_2\text{O}$  [5]. At the inflection point  $h = J_{\perp}$  the magnetization is 0.5. The curve is in excellent agreement with the experimental result [5].

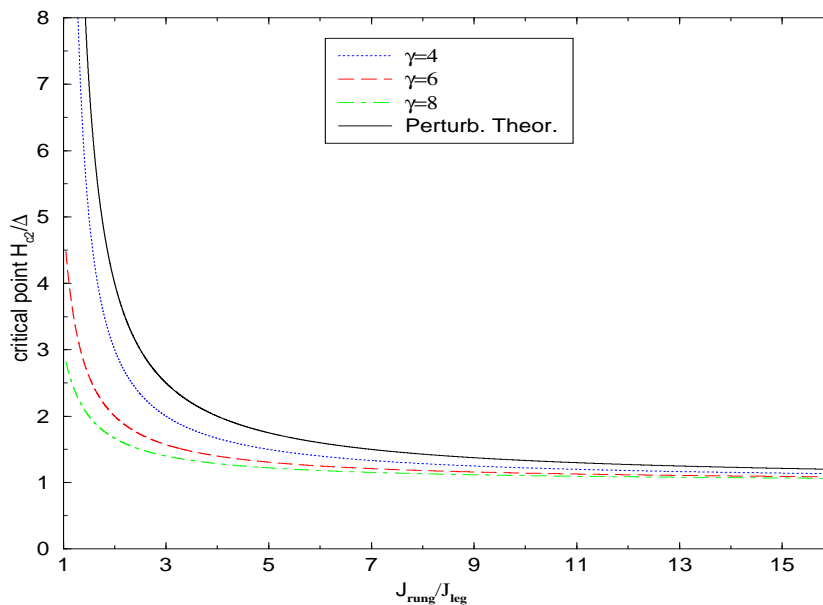


**Figure 2.** The critical point  $H_{c2}/\Delta$  as a function of the ratio  $J_{\perp}/J_{\parallel}$  for different values of the rescaling parameter  $\gamma$ . Also shown is the perturbation theory result.



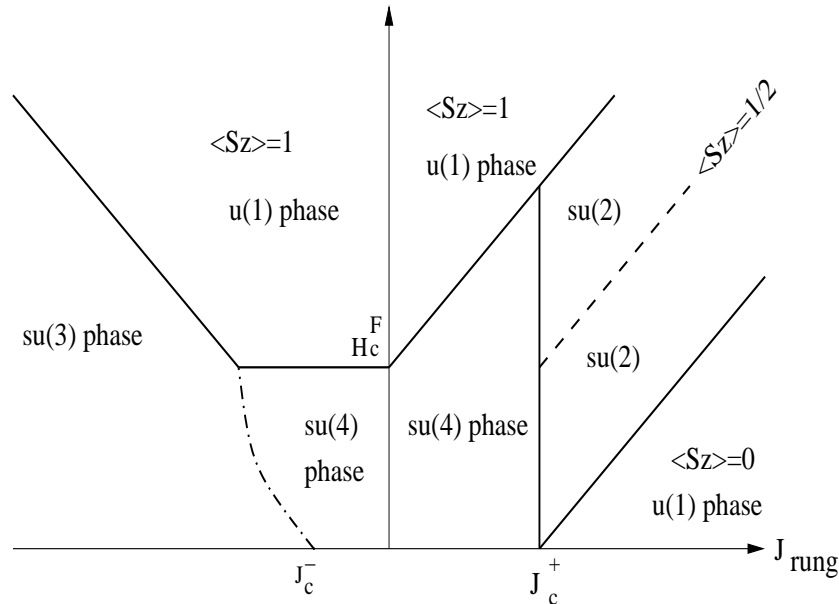


**Figure 3.** The magnetic phase diagram of the two-leg  $su(4)$  ladder. In the antiferromagnetic regime the thick lines are  $h = J_{\perp} - 4J_{\parallel}/\gamma$ ,  $h = J_{\perp} + 4J_{\parallel}/\gamma$  and the dash line is  $h = J_{\perp}$ . In the ferromagnetic regime the thick lines are  $h = -J_{\perp}$  and  $h = 4J_{\parallel}/\gamma$ . The dash-dot line is an approximate boundary between the  $su(4)$  and  $su(3)$  phases.

## Acknowledgments

The authors thank the Australian Research Council for support. A.F. and X.W.G. thank I. Roditi and Z.-J. Ying for helpful discussions as well as FAPERGS for financial support.

- [1] Dagotto E and Rice T M 1996 *Science* **271** 618  
Dagotto E 1999 *Rep. Prog. Phys.* **62** 1525
- [2] Azuma M, Hiroi Z, Takano M, Ishida K and Kitaoka Y 1994 *Phys. Rev. Lett.* **73** 3463
- [3] Chaboussant G *et al* 1997 *Phys. Rev. Lett.* **79** 925  
Chaboussant G *et al* 1998 *Phys. Rev. Lett.* **80** 2713  
Chaboussant G *et al* 1997 *Phys. Rev.* **B55** 3046
- [4] Watson B C, Kotov V N and Meisel M W 2001 *Phys. Rev. Lett.* **86** 5168
- [5] Landee C P, Turnbull M M, Galeriu C, Giantsidis J and Woodard F M 2001 *Phys. Rev.* **B63** 100402
- [6] Tanaka H, Takatsu K, Shiramura W and Ono T 1996 *J. Phys. Soc. Japan* **65** 1945  
Nakamura T and Okamoto K 1998 *Phys. Rev.* **B58** 2411
- [7] Shiramura W *et al* 1997 *J. Phys. Soc. Japan* **66** 1900
- [8] Nersesyan A A and Tsvetik A M 1997 *Phys. Rev. Lett.* **78** 3939  
Kolezhuk A K and Mikeska H-J 1998 *Phys. Rev. Lett.* **80** 2709
- [9] Zheng W, Singh R R P and Oitmaa J 1997 *Phys. Rev.* **B55** 8052
- [10] Dagotto E, Riera J and Scalapino D 1992 *Phys. Rev.* **B45** 5744
- [11] Reigrotzki M, Tsunetsugu H and Rice T M 1994 *J. Phys. Condens. Matter* **6** 9235  
Giamarchi T and Tsvetik A M 1999 *Phys. Rev.* **B59** 11398

- [12] Totsuka K 1998 Phys. Rev. **B57** 3454 Barnes T and Riera J 1994 Phys. Rev. **B50** 6817.
- [13] Wang Y 1999 Phys. Rev. **B60** 9236
- [14] Batchelor M T and Maslen M 1999 J. Phys. A **32** L377  
Frahm H and Kundu A 1999 J. Phys. C: Cond. Mat. **11** L557  
de Gier J, Batchelor M T and Maslen M 2000 Phys. Rev. **B61** 15196  
Batchelor M T, de Gier J and Maslen M 2001 J Stat. Phys. **102** 559  
Maslen M, Batchelor M T and de Gier J, cond-mat/0302135.
- [15] Park S and Lee K 1998 J. Phys. A: Math. Gen. **31** 6569
- [16] Johnston D C, Johnson J W, Goshorn D P and Jacobson A J 1987 Phys. Rev. **B35** 219
- [17] Hayward C A and Poilblanc D 1996 Phys. Rev. **B54** R12649
- [18] Sutherland B 1975 Phys. Rev. **B12** 3795  
Schlottmann P 1992 Phys. Rev. **B45** 5293
- [19] M. Takahashi 1971 Prog. Theor. Phys. **46** 401  
P. Schlottmann 1986 Phys. Rev. **B33** 4880.
- [20] K. Lee 1994 J. of the Korean Phys. Soc. **27** 205.
- [21] de Gier J and Batchelor M T 2000 Phys. Rev. **B62** R3584  
Cai S, Dai J and Wang Y 2002 Phys. Rev. **B66** 134403
- [22] Troyer M, Tsunetsugu H and Würtz D 1994 Phys. Rev. **B50** 13515
- [23] Chaboussant G *et al* 1998 Eur. Phys. J. B **6** 167